Food Chemistry: X 22 (2024) 101512

Contents lists available at ScienceDirect

Food Chemistry: X

journal homepage: www.sciencedirect.com/journal/food-chemistry-x

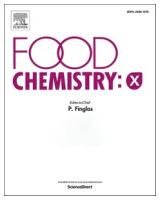

Moderation-excess interactions of epigallocatechin gallate and $CaCl_2$ modulate the gelation performance of egg white transparent gels

Weiling Chen [a,*], Xingtian Chen [c], Wenjing Liang [a], Huiqing Liao [a], Haisang Qin [a], Bangdong Chen [a], Minmin Ai [b,*]

[a] Guangxi Key Laboratory of Health Care Food Science and Technology, College of Food and Bioengineering, Hezhou University, Hezhou 542899, China
[b] The National Center for Precision Machining and Safety of Livestock and Poultry Products Joint Engineering Research Center, College of Food Science, South China Agricultural University, Guangzhou 510642, China
[c] College of Materials and Chemical Engineering, Hezhou University, Hezhou 542899, China

ARTICLE INFO

Keywords:
Epigallocatechin gallate
Calcium ion
Egg white protein
Gelation performance
Digestive behavior

ABSTRACT

In this study, the moderation–excess interaction of epigallocatechin gallate (EGCG) and calcium ions (Ca^{2+}) to the gelation performance of transparent egg white protein (EWP) gel (EWG) was explored. The oxidation of EGCG introduced a yellowish-brown EWG, whereas the weakening of Ca^{2+} ionic bonds caused a notable reduction in the hardness of EWG, from 120.67 g to 73.57 g. Achieving the optimal EGCG-to-Ca^{2+} ratio in EWG conferred enhanced water-holding capacity to 86.98%, while an excess of EGCG attributed to the creation of a three-dimensional structure within the void "walls". The elevated presence of EGCG influenced the ionic bonds and hydrophobic interactions, thereby presenting a moderate–excess relationship with sulfhydryl and disulfide bonds, β-sheet, and α-helical structures. Notably, EGCG reduced the digestibility of EWG to 50.06%, while concurrently fostering the creation of smaller particle sizes. This study provides a scientific basis for the controllable preparation and quality regulation of transparent EWG.

1. Introduction

Egg white (EW) is the main component of eggs, showing a natural weak gel aggregation in a transparent state, which is directly related to the variation of egg quality (Razi, Fahim, Amirabadi, & Rashidinejad, 2023). EW protein (EWP) forms different gels under different conditions, particularly in the food industry being heat denaturation–induced turbid gels, such as poached and steamed eggs, and transparent gels with other processing aids, such as preserved EW or alkali-induced gels (Zhang et al., 2023). When EW is exposed to heat treatment, the three-dimensional structure of ovalbumin begins to unravel, and hydrogen bonds and non-covalent interactions are broken, leading to the cross-linking and polymerization of protein chains (Liu et al., 2020). The cross-linked protein chains form a stable network structure that solidifies into an opaque gel, trapping water and other solutes in the gel structure to form a robust structure. EWP induced by alkaline denaturing reagents, such as NaOH, results in the opening of its secondary structure. This process leads to an increase in OH^- ions, the breaking of hydrogen bonds, and an increase in hydrophilic groups. As a result, a large amount of free water becomes bound water, and a three-dimensional network structure is formed through programmed cross-linking with proteins via hydrophobic interactions and other forces. However, excessive alkali leads to excessive ionic bond strength and pH, the internal chemical bond balance of the transparent gel was broken with gel structure collapses (Gao et al., 2020). Furthermore, an imbalance between the rate of protein aggregation and denaturation regulates the transparency of EWP gel (EWG). However, the mechanism underlying transparent EWG is not clearly defined, and egg scientists are still trying to analyze the specific mechanism.

Epicatechin gallate (EGCG) is a tea polyphenol with antioxidant properties and a variety of potential health benefits (Li & Chen, 2022). The molecular structure of EGCG consists of a benzene ring and a monomer of catechin, with a gallic acid group (gallate; Nagle, Ferreira, & Zhou, 2006). Black tea powder, enriched with EGCG, is added to the curing solution in the preparation of preserved eggs, which imparts a deep reddish-brown color. Although EGCG tends to oxidize under alkaline conditions to form polymers affecting protein stability, leading to protein precipitation, structural and color changes, and antioxidant

* Corresponding authors.
E-mail addresses: chenchenweiling@163.com (W. Chen), scauaiminmin@scau.edu.cn (M. Ai).

https://doi.org/10.1016/j.fochx.2024.101512
Received 29 March 2024; Received in revised form 15 May 2024; Accepted 25 May 2024
Available online 27 May 2024

properties (Xu, Yu, & Zhou, 2019). The antioxidant properties of EGCG decelerate the oxidative reactions of EWP under alkaline conditions and maintain and prevent the original structure of EWP from being damaged by alkali (Xue, Luo, Tu, Zhao, & Zhang, 2023). Certainly, EGCG, as a dietary probiotic factor, is loaded by applying various embedding materials to enhance the stability of EGCG, and the hydrogel formed by EWP, as a common and effective delivery vehicle, is interfered by EGCG regarding the gel properties (Tan et al., 2022). However, it is not clear how the interaction of EGCG with EWP would affect the transparency of alkali induced EWG and how it would modulate the digestive behavior of the gels as gelatinous foodstuffs.

Ca^{2+} is frequently applied in many food preparations, especially dairy and soy products. Ca^{2+} is gel cross-linking mediating reagents that promote gel formation, which improves the texture and structure of food products by interacting with anions in proteins to form gel network structures (Liang et al., 2020). The presence of Ca^{2+} enhances gel stability and prevents gel disintegration (Wang et al., 2020). The hardness and texture of the food gel can be controlled to match the specific product requirements by adjusting the concentration and addition time of Ca^{2+} (Xiao et al., 2021). The addition of tea polyphenols (mostly EGCG) to alkali induced EWG has been reported to demonstrate a reduction in gel properties (Ai et al., 2019). Whereas lime is added to the pickling solution of traditional preserved egg-transparency gels, which contains Ca^{2+} that definitely affects the strength of EWG, it is not clear about how EGCG and Ca^{2+} synergistically influence the performance of EWG. And the phenolic group in EGCG can form complexes with Ca^{2+} under alkaline conditions, leading to structural changes in EGCG, thus affecting its solubility and activity, and it is not clear whether synergistic or inhibitory effects occur. Therefore, the structure and properties of protein-Ca^{2+}-EGCG complexes in the formation of EWG must be studied in greater depth to understand how the complex modulates the formation and properties of EWG.

Hence, in this study, we directly induced the formation of EWG by directly adding NaOH using an off-shell model; investigated the effects of different ratios of EGCG and Ca^{2+} on the stability and physicochemical properties of EWP solution; analyzed the gel properties the prepared EWG; and characterized the digestive behavior to fully elucidate the mechanism of the moderation-excess effects of EGCG and Ca^{2+} on EWP gelation performance. This study is based on the deep excavation of traditional egg product processing, and the results will lay a theoretical foundation for the precise control of preserved eggs quality and provide a scientific basis for the controllable preparation of EWG.

2. Material and methods

2.1. Materials

Eggs were purchased from a supermarket in Guangzhou, China. Trypsin was purchased from the Shanghai Yuanye Biotechnology Company (Shanghai, China). EGCG were purchased from Aladdin Reagent Corporation (Shanghai, China). $CaCl_2$ was obtained from Tianjin Chemical Technology Co., Ltd. (Tianjin, China). 8-Aniline-1-naphthalenesulfonic acid (ANS) was supplied from Sigma (St. Louis, MO, USA). Other chemical reagents were of analytical grade.

2.2. Interaction among EGCG, $CaCl_2$, and EWP

Fresh eggs were washed with tap water and dried. The EW and yolks were separated and obtained EWP, adjusted EWP to 10 mg/mL, and a mixture of EGCG and $CaCl_2$ with a total amount of 0.04% (w/w) was added to 100 mL of EW (ratios of $CaCl_2$: EGCG = 0:1, 1:4, 2:3, 1:1, 3:2, 4:1, respectively); 1 mol/L NaOH was used to adjust the pH of reaction system, the pH values were 7.0, 9.0, and 11.0; and dispersed homogeneously at 1,000 ×g for 30 min to obtain EWP-EGCG-$CaCl_2$ complexes by homogeneous dispersion.

2.2.1. Particle size, ζ-potential, and turbidity

The EWP-EGCG-$CaCl_2$ complexes were diluted into 1 and 0.1 mg/mL with 50 mM of sodium phosphate-buffered solution at different pH. The average particle size (1 mg/mL) and ζ-potential (0.1 mg/mL) were determined (Zetasizer Nano ZS-90, Malvern Instruments, Worcestershire, UK) over 12 cycles before being equilibrated for 2 min. The average particle size and ζ-potential of complexes were collected. The protein content of EWP conjugates was diluted to 2 mg/mL, and the absorbances were measured at 500 nm using a spectrophotometer (UV2600, Shimadzu, Tokyo, Japan).

2.2.2. Surface hydrophobicity

The surface hydrophobicity of EWP-EGCG-$CaCl_2$ was determined as described in our previous study (Ai & Jiang, 2021). In brief, added 20 μL of 8 mM ANS solution to the complex solution with concentrations of 0.5, 1, 1.5, 2, and 2.5 mg/mL, and reacted in the dark for 15 min, with excitation and emission at 390 and 470 nm, respectively. Absorbance values were measured (RF-5301PC, Shimadzu, Tokyo, Japan), and the surface hydrophobicity was determined by calculating the slope of a one-time correlation between the absorbance value and complex concentration.

2.3. Preparation of EWG

Alkali-induced EWG was prepared in accordance with the method described in our previous studies (Ai & Jiang, 2021). In brief, after conjugation at pH 9.0, 20 mL of EW and 1 mL of NaOH solution (1.14%, w/w) were mixed quickly to achieve mixtures with 0.57% NaOH and stored at 4 °C overnight to allow the gels to reach equilibrium.

2.4. Textural properties

Texture property analysis was conducted using a TA-XT Plus texture analyzer (Stable MicroSystems, Surrey, UK). Textural profile analysis was performed, and the samples were prepared at 10 mm^3 with a knife and compressed to 50% of the original height with 1 mm/s pretest and test speed fitted with a probe of P/36R. The hardness, gumminess, resilience, and springiness were also calculated.

2.5. Water-holding capacity (WHC)

The WHC of the EWG was determined in accordance with the method of Li et al. (2018) with slight modifications. A dry filter paper was lined at the bottom of the centrifuge tube, and then 3 *g* of EWG was placed in the centrifuge tube and centrifuged at 15,000 ×*g* for 10 min. The EWG was removed, and the difference in weight between the centrifuge tube and filter paper before and after the centrifugation was weighed to calculate the WHC of the EWG.

2.6. Color

A volume of 1 cm^3 EWG was laid flat on the test plate, and the L^*, a^*, and b^* values of the EWG were determined by using a colorimeter (SP62, X-Rite corporation, Michigan, USA) after correction for black and white boards, and the ΔE value ($\Delta E = \sqrt{\left(L^{*2} + a^{*2} + b^{*2}\right)}$) was calculated.

2.7. Low field nuclear magnetic resonance (LF-NMR)

Following a previous study (Chen, Zou, Zhou, Liu, & Benjakul, 2023), the mobility and distribution of water molecules in the EWG were analyzed using a LF-NMR analyzer (LF-NMR, MesoMR23-040 V-I, Niumang Analytical Instrument Corporation, Shanghai, China). Specimens from each treatment (15 mm internal diameter, 20 mm length) were placed in a nuclear magnetic resonance tube (40 mm) and analyzed in

five parallel runs at 32 °C. Carr-Purcell-Meiboom-Gill sequences with a τ value of 250 μs were used to measure T_2. A total of 3000 echoes were acquired with 16 repetitions. Data were analyzed using MultiExp Inv Analysis (Niumag Electric Corporation, Shanghai, China).

2.8. Fourier transform infrared spectroscopy (FTIR)

The infrared spectrum of EWG was determined using a FTIR spectrometer (Bruker vertex70, Coventry, Germany). 1.2 mg of dried EWG powder and 100 mg KBr were ground in an agate mortar and assessed in the range of 4000–400 cm^{-1} using 16 scans at 4 cm^{-1} resolution. Pure KBr was used as the reference.

2.9. Dominant bonds

2.9.1. Sulfhydryl (SH) and disulfide (SS) bonds

The content of SH and SS bonds was measured in accordance with the method described in our previous study (Ai et al., 2020). After centrifugation, the supernatant was obtained by dispersing 3 g EWG in 27 mL sodium phosphate buffer (0.1 mol/L pH 8.0). For the determination of free SH content (SH_F), 0.2 mL of supernatant was mixed with 2.8 mL of 20 mmol/L Tris-gly buffer (pH 8.0, containing 0.004 mol/L ethylenediamine tetraacetic acid and 8 mol/L urea) and 0.02 mL of Ellman's reagent (4 mg/mL of 5,5'-Dithiobis-(2-nitrobenzoic acid) dissolved in Tris-gly buffer) at 40 °C in a water bath for 15 min, and the absorbance was measured at 412 nm (UV2600, Shimadzu, Tokyo, Japan). In determining total SH content (SH_T), 0.2 mL of supernatant was incubated with 2.8 mL of 20 mmol/L Tris-Gly buffer (pH 8.0, containing 1.5 mg/mL of β-mercaptoethanol, 0.5% sodium dodecyl sulfate, and 8 mol/L urea) at 40 °C in a water bath for 15 min. Then, 3 mL of 12% trichloroacetic acid was added and allowed to stand for 1 h at 40 °C. The precipitate was collected by centrifugation at 5000 ×*g* for 10 min and washed three times with 12% trichloroacetic acid solution. Next, 2.8 mL of 20 mmol/L Tris-gly buffer (pH 8.0) and 0.02 mL of Ellman reagent were added to dissolve the precipitate in water baths at 40 °C for 15 min, and the resulting mixture was then analyzed spectrophotometrically in accordance with the method used for SH_F. An extinction coefficient of 13,600 M^{-1} cm^{-1} was used to calculate the SH content, and the SS bonds was calculated as half of SH_T minus SH_F content.

2.9.2. Solvent protein fractions

Intermolecular forces were determined in accordance with the method described by Gómez-Guillén, Borderías, and Montero (1997), and disperse the 2 g sample into 10 mL five kinds of solution: 0.06 mol/L NaCl, 0.6 mol/L NaCl, 0.6 mol/L NaCl +1.5 mol/L urea, 0.6 mol/L NaCl +8 mol/L urea, and 0.6 mol/L NaCl +8 mol/L urea +1.5% β-mercaptoethanol. The difference among solvents represents various intermolecular interactions.

2.10. Scanning electron microscopy (SEM)

The microstructure was observed by SEM (Quanta-200F, FEI, Netherlands). 0.5 g of EWG was soaked in sodium phosphate buffer (100 mM, pH 7.2) containing 2.5% glutaraldehyde for 30 min, then soaked for 15 min using sodium phosphate buffer solution three times, freeze dried, and then photographed by 200-fold at 5 kV to visualize the morphological structure.

2.11. Digestion behavior

In studying the digestive behavior of EWG, an in vitro simulated digestion model consisting of sequential gastric (60 min) and intestinal (120 min) digestions was adopted. In brief, 5 g of EWG was pre-incubated in a shaker (at 37 °C) at 100 rpm for 10 min by mixing well with 100 mL of simulated gastric fluid (pH 1.5). Then, simulated gastric digestion was initiated by adding 80 mg of pepsin powder (60 U/mL) and mixing well. After 60 min, the pH of the pepsin digest was immediately adjusted to 7.0 with 4 mol/L of NaOH, and 2 g of bile extract was added and shaken well for 10 min. Finally, to start the intestinal digestion (60–180 min), 200 mg of pancreatin powder (100 U/mL) was added. At the end of the digestion, 0.5 mL of the final digestion dispersion was collected and centrifuged at 10,000 ×*g* for 15 min. The absorbance of the supernatant after centrifugation was measured using the bovine serum protein standard curve. The concentration of protein in the digested fluid during digestion was determined. The ζ-potential and average particle size of the digested EWG were measured as described in Section 2.2.1.

2.12. Statistical analysis

The differences among the mean values were compared with using SPSS software 21.0, and the significant difference was shown as $P < 0.05$. Each assay was performed at least three times.

3. Results and discussion

3.1. Covalent interaction of EWP-EGCG-$CaCl_2$

The average particle size and ζ-potentials of the EWP-EGCG-$CaCl_2$ complex at different pHs are shown in Fig. 1A and B. The particle size of the complexes decreased significantly with the increase in the ratio of EGCG ($P < 0.05$), with the largest particle size at $CaCl_2$:EGCG = 4:1, the particle size of the complex at pH 9.0 was significantly higher than that at pH 7.0 and pH 11.0 ($P < 0.05$), and the strong alkalinity caused denaturation of EWP. The surface charge of the complexes formed under neutral conditions was low, whereas the absolute value of ζ-potential increased significantly with the growth of pH ($P < 0.05$), which increased initially and then decreased with the increase of EGCG ratio. Under alkaline conditions, EGCG may bind with cations in the solution, thereby affecting the surface charge of the complex. Ca^{2+} interacts with protein phosphates to produce insoluble aggregation (Miao et al., 2023) and forms aggregates with a larger particle size (Fig. 1A), which is similar to a previous study (Alavi, Tian, Chen, & Emam-Djomeh, 2020). $CaCl_2$ promoted the aggregation of preheated EWP. Furthermore, Ca^{2+} induced bridging among proteins and increased the particle size of protein aggregates, whereas EGCG covalently interacted with EWP to form structurally stable complexes and further mediated by Ca^{2+} to form EWP-EGCG-Ca^{2+} covalent aggregates, which showed a significant decrease in particle size compared with the high proportion of Ca^{2+}. The sheltering effect of the positive charge of Ca^{2+} decreased the negative charge on the surface of the complexes, whereas the complexation of EGCG with the proteins exposed more anionic groups, which increased the negative charge (Fig. 1B), indicating a more stable system.

The turbidity of EWP-EGCG-$CaCl_2$ complexes is shown in Fig. 1C. At pH 7.0, the turbidity of the complexes initially increased and then decreased. However, for complexes at pH 9.0, the turbidity decreased gradually as the proportion of EGCG proportion increased, and the turbidity of the complex at pH 11.0 showed irregular variations. The results showed that the binding and aggregation states of EWP-Ca^{2+}-EGCG varied in different pH environments, and the formation of the complexes resulted in differences in turbidity because of the competing pH responses of hydrogen bonding in EGCG and ionic bonding in Ca^{2+} (Zhang et al., 2023). Chen, Zhou, Gao, Wu, and Liang (2022) applied EGCG to treat zein and found that negatively charged EGCG could electrostatically neutralize the positively charged interactions on the surface of zein colloidal nanoparticles and further attenuate the electrostatic repulsion. By contrast, in our study, the electrostatic interaction between EGCG and proteins was unstable because of Ca^{2+} competition particularly under alkaline conditions.

The changes in surface hydrophobicity are shown in Fig. 1D. The surface hydrophobicity values increased significantly with the increase of EGCG ratio, reaching the maximum at the highest EGCG ratio, and the

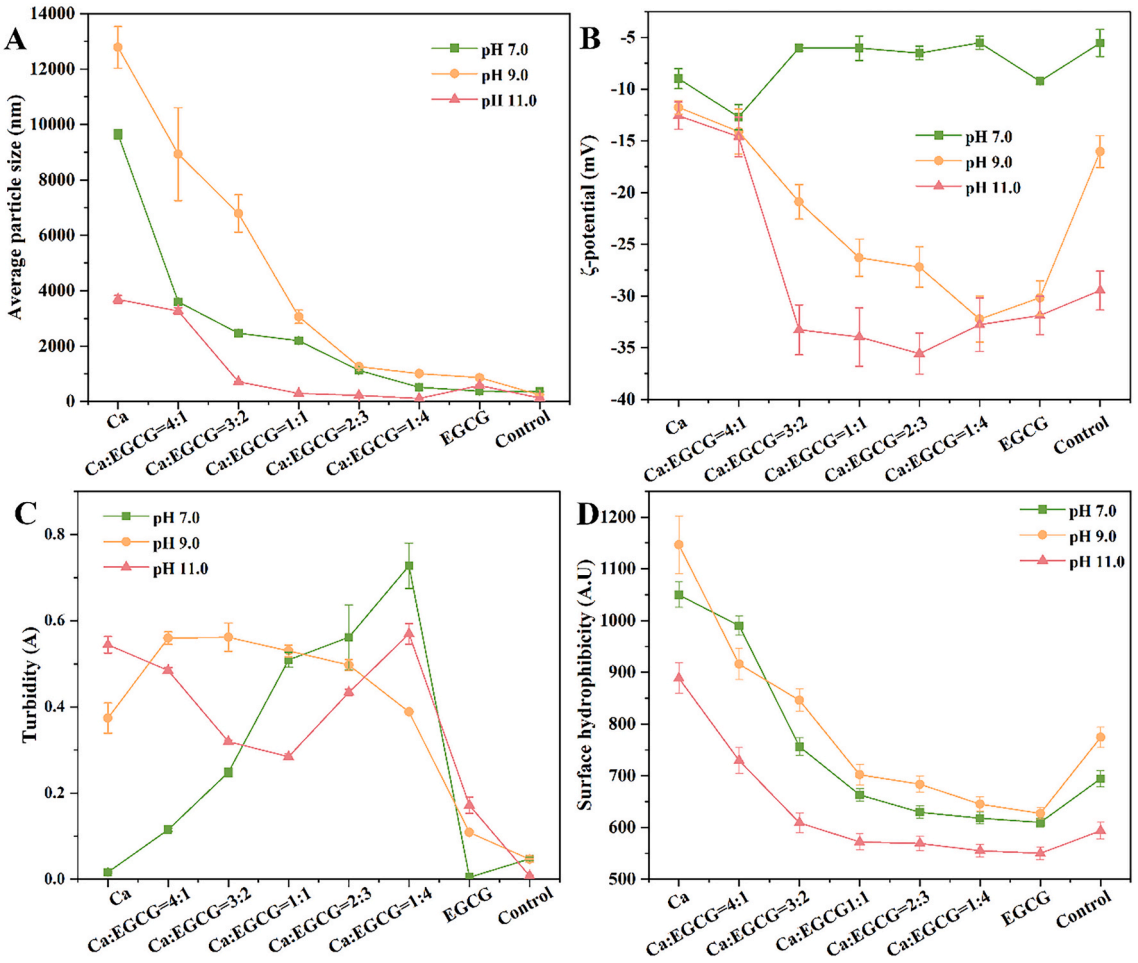

Fig. 1. The particle size (A), ζ-potential (B), turbidity (C) and surface hydrophibicity (D) of EWP as affected by different ratio of EGCG and $CaCl_2$ at pH 7.0, 9.0 and 11.0. Different letters for the same indicator mean significant difference ($P < 0.05$).

surface hydrophobicity at pH 9.0 was significantly higher than that at pH 7.0 and 11.0. Changes in surface hydrophobicity are associated with protein conformation and aggregation, and an increase in surface hydrophobic amino acid residues improves water-amino acids interactions while achieving protein stabilization. Combined with previous analysis of turbidity, proteins formed complexes with EGCG-Ca^{2+} (Fig. 1C), and the hydrophobic groups on the surface were gradually encapsulated, whereas in the presence of EGCG, the effective aggregates were formed in a more dispersed manner, with an increased hydrophilic proportion and enhanced solubility. In addition, EGCG can effectively interact with protophilic groups on the surface of EWP, competitively avoiding contact with ANS and leading to a decrease in surface hydrophobicity (Gao et al., 2020). On the contrary, Ca^{2+} competes for water molecules, promoting protein contact with ANS and forming more amorphous complexes (Miao et al., 2023). In the weak alkaline condition, the interaction of EGCG, Ca^{2+} and EWP formed large particle complex, and the hydrophobic group on the surface of EW was embedded, and the interaction with water molecules was reduced. In the strong alkaline condition, the denaturation hydrolysis of EWP was dominant, although the polyhydroxy group of EGCG and the ionic action of Ca^{2+} had polymerization adhesion, showing a decrease in particle size and turbidity.

3.2. Textural properties of EWG

The textural properties of the EWG are shown in Fig. 2A and B. The hardness and gumminess value of the EWG decreased evidently with the increase of EGCG ratio ($P < 0.05$), which was contrary to the textural results of heat-induced EWG with the addition of EGCG (Xue et al., 2023), but consistent with the textural changes in the EWG with the addition of tea polyphenols (Ai & Jiang, 2021). The springiness value changed non-significantly when the percentage of the EGCG ratio was <0.02%, and the resilience value initially increased and then gradually decreased, reaching the maximum value at Ca:EGCG = 3:2.

The abundant hydroxyl groups and reactive double bonds in EGCG are deprotonated by hydroxyl groups under alkaline conditions, leading to the formation of peroxides and oxidation products (Zeng, Ma, Li, & Luo, 2017), which form copolymers with proteins through hydrogen bonding and electrostatic interactions, and the results was consistent with the changes in turbidity and ζ-potential showed in Fig. 1B and C. However, the weak interactions between EGCG oxides and protein copolymers are further attacked by the excessive OH-, leading to a significant decrease in hardness and chewiness. The addition of Ca^{2+} robes water molecules that are hydrogen bonded to proteins to form “calcium bridges”, forming a dense protein structure that enhanced the hardness and chewiness. Ca^{2+} and EGCG showed a substitution reaction, forming complexes, crosslinking with proteins, and more rigid areas to protect the gel from restoring its original form. In compression, the rigid structure formed slowly once again, so the resilience is low, and the excessive proportion of EGCG will further disrupt the equilibrium.

3.3. WHC and LF-NMR of EWG

The WHC of EWG is shown in Fig. 2C. The WHC increased initially and then decreased gradually with EGCG addition, and the maximum

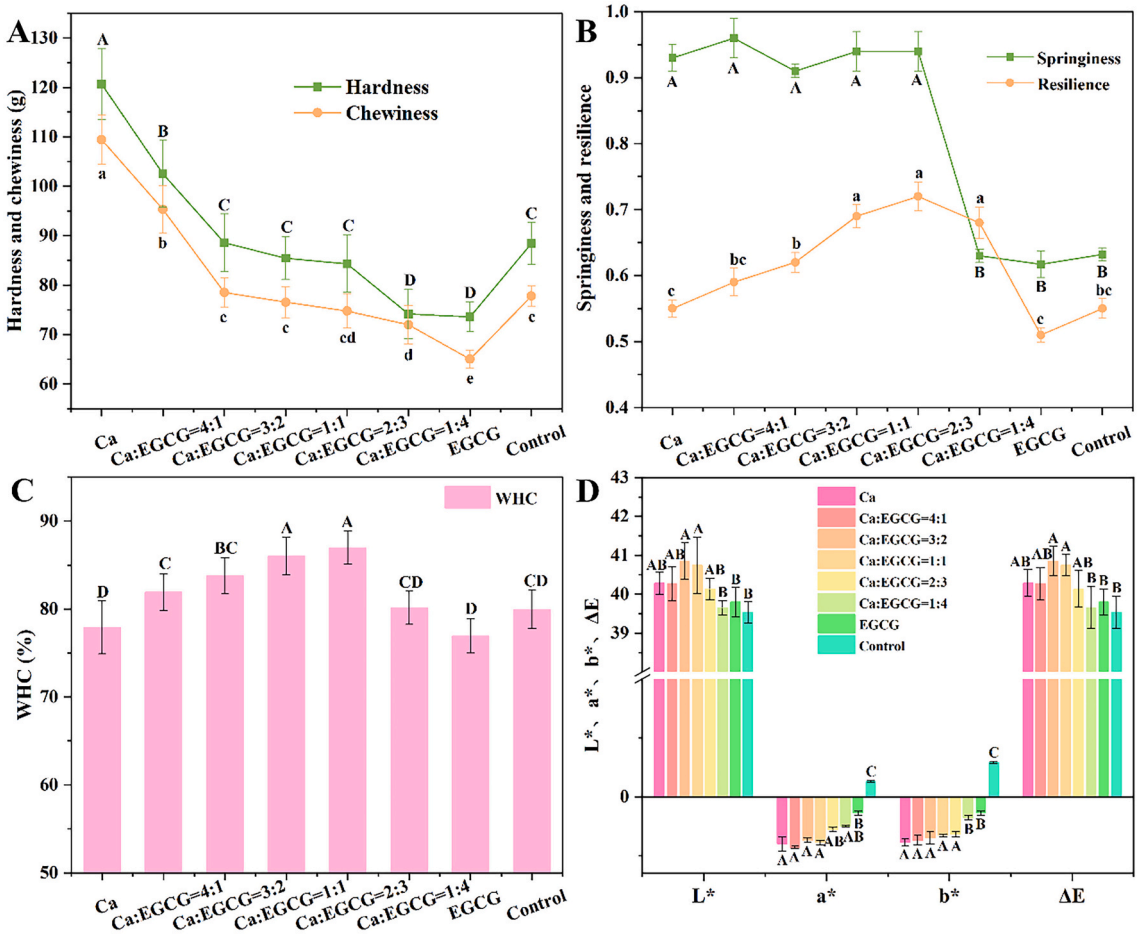

Fig. 2. The hardness and chewiness (A), resilience and springiness (B), the WHC (C) and color (D) of EWG as affected by different ratio of EGCG and $CaCl_2$. Different letters for the same indictor indicate significant difference ($P < 0.05$).

value, 86.98%, was achieved at Ca:EGCG = 1:1. In addition, the smallest value of WHC was observed in the group with only EGCG, which is consistent with our previous study (TP-ethanol-induced EWG; Yao, Jiang, & Chen, 2020). The hydroxyl group of EGCG and the ionic action of Ca^{2+} will interact with proteins to bind free water molecules in EW, and the synergistic interactions of appropriate ratios of EGCG and Ca^{2+} enhance the conversion of free water molecules to bound water, whereas a high proportion of EGCG, despite the enhanced hydrogen bonding with EWP, tolerates the attack of high concentrations of OH^- with insufficient ability. Thus, the WHC was reduced at high ratios of EGCG, which is consistent with the findings of Ji et al. (2024).

LF-NMR provides useful information about the interactions between exchangeable protons and water protons in proteins, which can be applied to analyze the distribution of water molecules (Gouda, Zhang, Liu, Sheng, & Ma, 2017). The LF-NMR results of EWG with added EGCG-Ca^{2+} are shown in Fig. 3C and D. All T_2 peaks, including T_{2b}, T_{21}, and T_{22}, among which T_{22} showed the highest peak and T_{2b} presented the lowest peak, and all the peak times initially increased and then declined with the improvement of EGCG proportion. T_{2b} and T_{21} achieved the maximum value at Ca:EGCG = 2:3 and the maximum peak of T_{22} at Ca:EGCG = 1:1. The T_{22} results were consistent with the previous changes in WHC (Yang, Zhang, Bhandari, & Liu, 2018). T_{21} refers to unfrozen water that binds tightly to large proteins, and T_{22} represents bound water in the gel network (Guo et al., 2019). The rotation and translation of water in the EWG formed by the synergistic action of EGCG with Ca^{2+} correlate with prolonged periods. Furthermore, a sustained increase in EGCG leads to an enhanced covalent interaction of the oxidation products with proteins, shifting toward longer relaxation times, which correlates with the microstructural densification of the gel. EGCG is highly hydrophilic, and its abundant hydroxyl group competes with water for interaction with proteins to draw bound water from protein molecules, and Ca^{2+} snatch up water molecules, co-regulating the state of water molecules in the gel. The distribution of water molecules in different states had a significant effect on the textural properties of EWG. From the textural properties, WHC and LF-NMR results, more water molecules in the bound state led to a stronger structural network of EWG, which revealed higher gel properties, whereas the different chemical interactions of Ca^{2+} and EGCG synergistically affected the water molecule state and regulated the gel state.

3.4. Appearance, color, and microstructure of EWG

The apparent features of EWG are shown in Fig. 3A. The brown coloration of EWG showed a correlation with increasing EGCG concentration, and the gel opacity increased with Ca^{2+} addition. The coloration of EWG with the addition of EGCG and $CaCl_2$ is shown in Fig. 2D. With the increase of the proportion of EGCG, the values of L^*, a^*, b^*, and ΔE were significantly decreased, which indicated that the oxidation of EGCG to form quinone compounds under strong alkaline conditions led to the deepening of the color and decrease of the transmittance. The addition of EGCG primarily causes the brown color of the added EGCG gel, as EGCG is highly unstable in neutral and alkaline aqueous solutions, and the hydroxyl deprotonation leads to the generation of peroxides and oxidation products and the subsequent formation of dimers (Krupkova, Ferguson, & Wuertz-Kozak, 2016). When only Ca^{2+} was added, light scattering showed opacity because of different

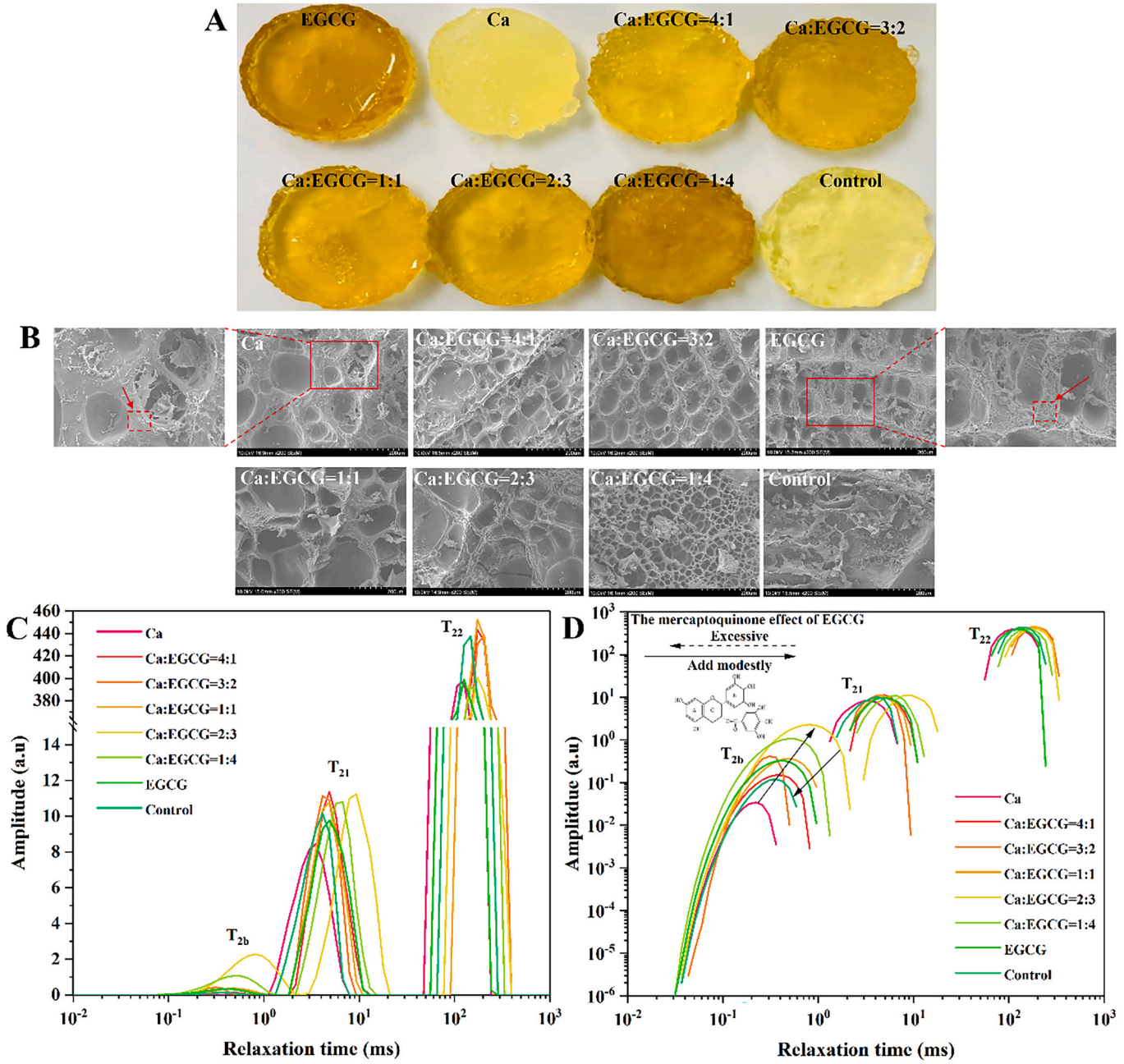

Fig. 3. The appearance features (A), SEM microstructure (B), and LF-NMR results, including un-logged (C) and logged (D), of EWG as affected by different ratio of EGCG and $CaCl_2$.

degrees of calcium bridges and protein aggregation.

EWP undergo alkaline denaturation and aggregation to form a three-dimensional network structure, and the network structure contributes to the textural properties of EWG. Therefore, SEM was applied to analyze the microstructure of EWG (Fig. 3B). The microstructures of all EWG showed a three-dimensional network structure, indicating that EWG exhibited well textural properties. When only Ca^{2+} was added, the proteins formed a strongly interconnected three-dimensional network driven by Ca^{2+}, and the thickness of the "wall" connections was strong. On the contrary, with the addition of EGCG, the "wall" connections were weakened, and more small pore structures were formed in the void "walls". This finding suggests that -OH in EGCG is hydrogen bonded to EW, resulting in the formation of abundant void-packet-void structures, particularly in the only EGCG addition group. Combined with the previous changes in textural properties and WHC, the strong supportive wall-connecting effect of Ca^{2+} enhanced the hardness and chewiness of EWG, whereas the cavity microstructure in the network structure-constructing walls weakened the textural properties of EWG. Our gel microstructure was more multidimensional, which caused the gel to exhibit translucent properties.

3.5. Dominant intermolecular forces of EWG

3.5.1. SH and SS bonds

The content of SH_F and SH_T content as well as SS bonds of EWGs is shown in Fig. 4A. The content of SH_F changed non-significantly ($P < 0.05$) before the Ca:EGCG = 2:3 ratio but increased significantly later ($P < 0.05$), except for the decreasement of the control group. The SH_T content and SS bonds initially increased and then decreased and obtained the maximum value at Ca:EGCG = 1:1. Ovalbumin is the main

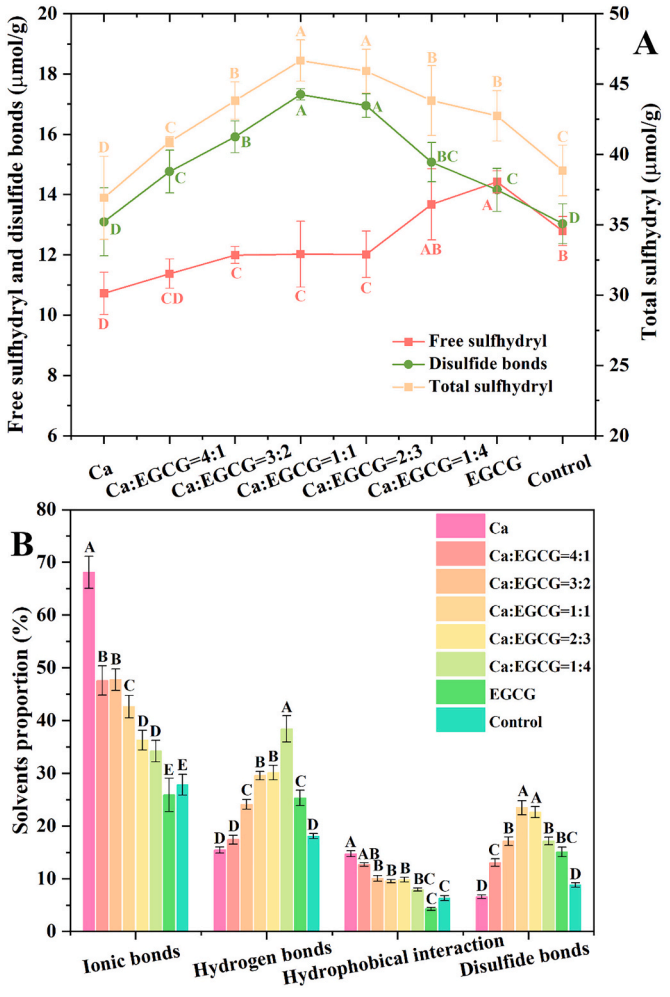

Fig. 4. The SH_T and SH_F contents, SS bonds content (A), intermolecular forces (B) of EWG as affected by different ratio of EGCG and $CaCl_2$. Different letters for the same indictor indicate significant difference ($P < 0.05$).

content in EWP, which was the only protein containing SH_F (Xue et al., 2022). During alkaline denaturation, ovalbumin was deacylated, and the four SH_F groups are susceptible to SS bonding or fracture transformation. With the increase of EGCG, the strongly reactive -OH and carbon–carbon double bond, which attacked the structured SH groups exposed, avoided the attack on the surface SH_F, which resulted in the decrease of the SH_T content. In addition, the imbalance between the SS-mercapto dynamic transition and the formation rate of the network structure during the gelation of EWP aggregates resulted in the encapsulation of more denatured proteins of the exposed SH. Combined with previous textural properties, the results indicated that Ca^{2+}-mediated salt bridging and the rigidity of SS bonds jointly regulate the gel properties of EWP. Combined with the previous structural properties, the results showed that Ca^{2+}-mediated salt bridging and the rigidity of SS together potentiated the gel properties of EWG, and that a high proportion of EGCG reduced the covalent cross-linking, inducing weak interaction between proteins and presenting lower textural properties and WHC.

3.5.2. *Intermolecular forces*

The dominant intermolecular forces of EWG are shown in Fig. 4B. With the decrease of the Ca^{2+} ratio, the proportion of ionic bonding decreased significantly ($P < 0.05$), and the proportion of hydrogen and SS bonds initially improved and then decreased, in which the hydrogen bonding achieved the maximum at Ca:EGCG = 1:4 with a maximum of 38.43%. In addition, the SS bonds changed consistently (Fig. 4A), and the maximum was achieved at Ca:EGCG = 1:1, reaching 23.48%. The proportion of hydrophobic interactions decreased gradually, which is consistent with the changes in surface hydrophobicity.

Our previous study found that the addition of tea polyphenols decreased the intermolecular forces, whereas adding $Ca(OH)_2$ enhanced the hydrogen bonding and hydrophobic interactions primarily (Ai et al., 2019). Combined with the previous results of the physical properties of EWG, EGCG effectively interfered with the ionic bonds and hydrophobic interaction of Ca^{2+}, and excessive EGCG affected the hydrogen and SS bonds, suggesting that EGCG alkaline-oxidized polymers are significantly less capable of affecting the textural properties than the ionic interactions dominated by Ca^{2+}, thereby leading to the reduction of hardness and chewiness (Fig. 2A). There are differences in the main forces to support different types of EWG, which influenced the physicochemical properties. Preserved egg, as a transparent EWG, was supported by ionic and SS bonds, whereas opaque boiled EWG was hold by hydrophobic interaction and SS bonds (Monge-Morera et al., 2020). The formation mechanism of EWG is relatively complex, and chemical forces effectively support the formation of EWG. The chemical properties of EGCG and Ca^{2+} are different, among which EGCG was easy to interact with EWP due to its rich phenolic hydroxyl group, hence, the rate of protein aggregation and denaturation was better regulated to form a transparent gel, and the electron layer of Ca^{2+} interacted with the protein to form a calcium bridge, resulting in different light scattering effects.

3.6. *FTIR, secondary structure, and three-dimensional spiral of EWG*

The FTIR of the EWG with added EGCG-Ca^{2+} is shown in Fig. 5A, which primarily demonstrates the absorbance values of 2000–400 cm^{-1}, exhibiting absorption peaks at 1627, 1485, 1383, and 1018 cm^{-1}, where 1627 cm^{-1} belongs to the amide I band from the C═O stretching (Han, Liang, Tian, Liu, & Wang, 2022), 1485 cm^{-1} from the CH_2 varved-angle vibration, 1383 cm^{-1} from the symmetric varved-angle of CH_3, and 1018 cm^{-1} from the C—O stretching (Bandyopadhyay, Ghosh, & Ghosh, 2012). When EGCG-Ca^{2+} and EWP interact, the modulation of intermolecular chemotactic forces intervenes in the changes of absorbing groups, such as C═O, CH_3, and CH_2. The changes in amide I bands indicated that EGCG and Ca^{2+} altered the secondary structure of the EWP. Ji et al. (2024) found that EGCG binds to proteins and perturbs -OH stretching vibrations and C═O stretching.

The secondary structure of EWG was analyzed, and the results are represented in Fig. 5B. β-sheet increased significantly before Ca:EGCG = 3:2 ($P < 0.05$) and decreased significantly at Ca:EGCG = 1:1 ($P < 0.05$), whereas β-sheet increased significantly as the proportion of EGCG increased later ($P < 0.05$). The random structure showed the lowest percentage and increased significantly with the addition of EGCG ($P < 0.05$). The α-helical content increased remarkably from 4.62% to 42.04% at Ca:EGCG = 1:1, whereas the percentage of β-turn decreased evidently from 60.05% to 18.04%, indicating that the β-turn of EWP is concentration-dependent with EGCG. Previous studies have reported that changes in β-sheet correlate with protein aggregation (Feng, Wang, Chen, & Wang, 2019), which in combination with the previous microstructural results may be related to the formation of wall microvoid structures, and that the enhanced "wall" void structure and water-binding encapsulation properties influence the modulation of the protein β-sheet structure by the EGCG-Ca^{2+} effects. The enhanced "wall" gap structure and binding water encapsulation properties affect the regulation of the protein β-sheet structure by EGCG-Ca^{2+}. Protein defolding significantly affected the functional properties of the proteins (Brown, Litvinov, Discher, Purohit, & Weisel, 2009), which was consistent with the changes in hardness and chewiness in the textural properties of EWG, which is in agreement with the previous study (Li et al., 2020). The three-dimensional helical structure was calculated by the helical/coil ratio (Fig. 5C). The ratio of three-dimensional helix

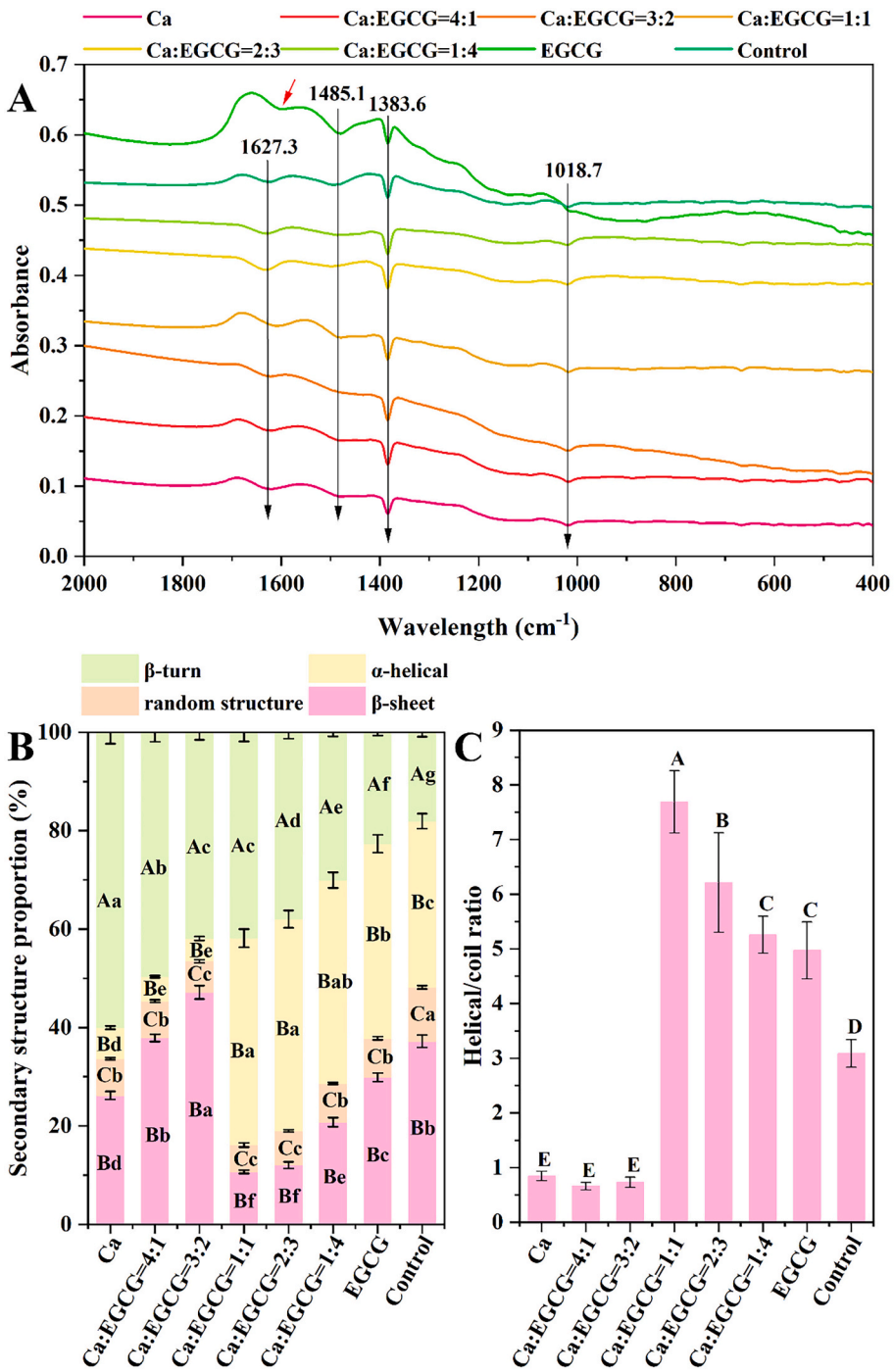

Fig. 5. The FTIR spectra (A), secondary structure (B) and helical/coil ratio (C) of EWG as affected by different ratio of EGCG and $CaCl_2$. Different letters for the same indictor indicate significant difference ($P < 0.05$).

ratios is consistent with the change in α-helical structures, indicating that hydrogen bonds modulated the formation of microstructures in EWG, and the structural strength of the entangled structure is reduced.

3.7. *In vitro digestion behavior of EWG*

The in vitro simulated digestion kinetics, the average particle size, and ζ-potential of EWG loaded with EGCG-Ca^{2+} are shown in Figs. 6A–E. In the simulated digestion, with the decrease of Ca^{2+} concentration, the digestibility decreased significantly ($P < 0.05$) and represented slower in the gastric digestion than intestinal digestion, indicating that EGCG affected the digestibility of EWG, which was related to the "mercapto-quinone" reaction between EGCG and EWP under alkaline conditions (Lv et al., 2019). The formation of chelates between EWG-EGCG-Ca^{2+} reduced the contact point of digestive enzymes. The average particle size of EWG after gastrointestinal digestion was correlated with the digestibility, and the EWG digestion was concentrated in the intestinal stage. The more pronounced the "void" structure of the wall of the three-dimensional structure formed, the lower the average particle size after digestion, indicating that EGCG caused the gel structure of EWG to disintegrate more easily. Similarly, EGCG was found to reduce the digestibility of water-soluble proteins probably because of the changes in gel strength and microstructure caused by the addition of EGCG (Santos et al., 2023).

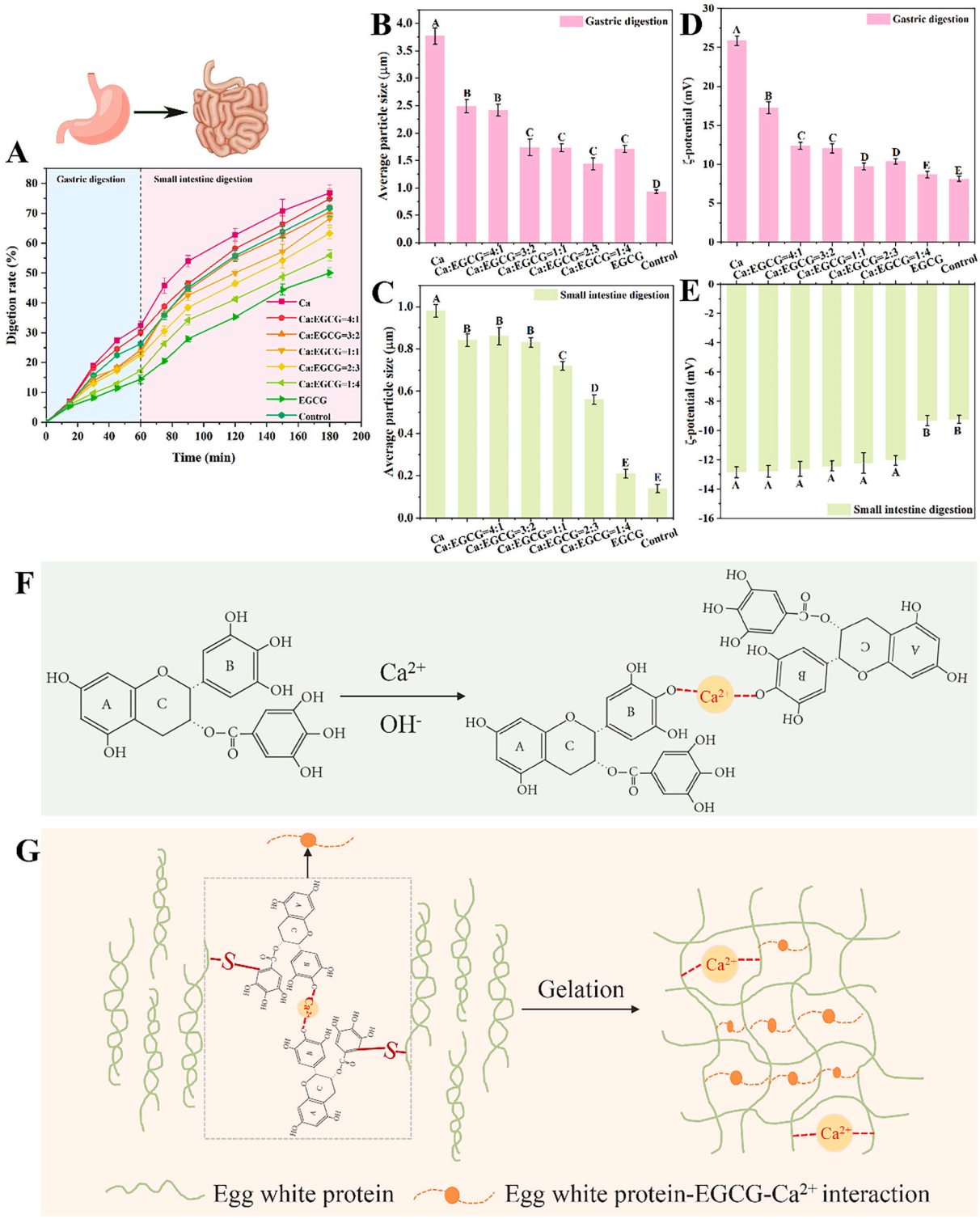

Fig. 6. The protein intestinal digestibility (A), digestive particle size (B) and ζ-potential (D) in the stomach, digestive particle size (C) and ζ-potential (E) in the small intestine of EWG as affected by different ratio of EGCG and $CaCl_2$. The possible mechanism of EGCG interacted with Ca^{2+} (F), and the interaction affects the gelation properties of EWP (G). Different letters for the same indictor indicate significant difference ($P < 0.05$).

The surface charge of the gel particles intervenes the digestion characteristics by influencing the aggregation behavior (Luo, Boom, & Janssen, 2015). During gastric digestion, the ζ-potential decreased with the increase of EGCG because of the strong acidic condition, which conferred more H^+ on the gel particles to exhibit a positive charge. After intestinal digestion, the ζ-potential showed a negative value, but the change was not significant with the addition of Ca^{2+} ($P < 0.05$), whereas the ζ-potential decreased significantly in the only EGCG addition group. Comparing all the physicochemical properties of the previous sections, the substitution reaction between EGCG and Ca^{2+} occurred in the proper proportion (Fig. 6F), and when interacting with proteins, EWP underwent structural transformation, resulting in different microstructures, which affected the cleavage effect of enzymes during digestion. Although the addition of EGCG limited protein digestion, possibly

because of the effective passivation of the enzyme by EGCG oxides, the reduction in particle size was due to the addition of EGCG, which promoted the formation of more loose structures, resulting in the exposure of controllable enzyme cleavage sites (Fathi, Donsi, & McClements, 2018). The digestion mode of EWG with the addition of excessive EGCG is primarily erosion, whereas fragmentation is the main digestion mode for the more Ca^{2+} addition group.

4. Conclusion

In this study, EGCG and Ca^{2+} were utilized to modulate the gelation properties and digestibility of EWP. The formed complex of EGCG and Ca^{2+} affected the ζ-potential and conformational morphology of EWP, resulting in varied aggregation patterns at different alkaline pH. The oxidation of EGCG imparted a yellowish-brown color to EWG, whereas the weakening of Ca^{2+} ionic bonds led to a substantial reduction in the hardness and chewiness of EWG. The optimal EGCG to the Ca^{2+} ratio in EWG conferred a stronger WHC, whereas excessive EGCG caused a decrease in WHC, which was associated with the formation of a three-dimensional structure in the void "walls." The increased EGCG levels affected the ionic bonds and hydrophobic interactions, as well as decreased the β-turn of the EWG in a moderate–excess relationship with SH and SS bonds, β-sheet, and α-helical structures. EGCG influenced the efficiency of digestive enzymes with the reduction of EWP digestibility, while concurrently creating smaller particle sizes. The findings of this project provide valuable insights into quality control in the production of transparent EWGs and provide a scientific foundation for designing food systems that rely on triple interactions. Certainly, to better achieve the precise regulation of EWG, the research on the interactions of EGCG and Ca^{2+} with specific proteins in EW and their effects on the properties of EWG can be further progressed, and can be developed in the direction of the design of gel foods for specific groups of people with particular needs.

CRediT authorship contribution statement

Weiling Chen: Writing – original draft, Investigation, Formal analysis. **Xingtian Chen:** Writing – original draft, Investigation, Formal analysis. **Wenjing Liang:** Investigation. **Huiqing Liao:** Investigation. **Haisang Qin:** Investigation. **Bangdong Chen:** Investigation. **Minmin Ai:** Writing – review & editing, Supervision, Resources.

Declaration of competing interest

The authors declare that they have no known competing financial interests or personal relationships that could have appeared to influence the work reported in this paper.

Data availability

Data will be made available on request.

Acknowledgment

This study was supported by department of education of Guangxi Autonomous Region (2020KY18019); Opening Project of Guangxi Key Laboratory of Health Care Food Science and Technology.

References

Ai, M., & Jiang, A. (2021). Phosphorylation modification affects the gelation behavior of alkali-induced duck egg white gels. *Food Chemistry, 340*, Article 128185.

Ai, M., Zhou, Q., Guo, S., Ling, Z., Zhou, L., Fan, H., … Jiang, A. (2019). Effects of tea polyphenol and ca(OH)$_2$ on the intermolecular forces and mechanical, rheological, and microstructural characteristics of duck egg white gel. *Food Hydrocolloids, 94*, 11–19.

Ai, M., Zhou, Q., Xiao, N., Guo, S., Cao, Y., Fan, H., … Jiang, A. (2020). Enhancement of gel characteristics of NaOH-induced duck egg white gel by adding ca(OH)$_2$ with/without heating. *Food Hydrocolloids, 103*, Article 105654.

Alavi, F., Tian, Z., Chen, L., & Emam-Djomeh, Z. (2020). Effect of $CaCl_2$ on the stability and rheological properties of foams and high-sugar aerated systems produced by preheated egg white protein. *Food Hydrocolloids, 106*, Article 105887.

Bandyopadhyay, P., Ghosh, A. K., & Ghosh, C. (2012). Recent developments on polyphenol–protein interactions: Effects on tea and coffee taste, antioxidant properties and the digestive system. *Food & Function, 3*(6), 592–605.

Brown, A. E., Litvinov, R. I., Discher, D. E., Purohit, P. K., & Weisel, J. W. (2009). Multiscale mechanics of fibrin polymer: Gel stretching with protein unfolding and loss of water. *Science, 325*(5941), 741–744.

Chen, H., Zou, Y., Zhou, A., Liu, X., & Benjakul, S. (2023). Elucidating the molecular mechanism of water migration in myosin gels of Nemipterus virgatus during low pressure coupled with heat treatment. *International Journal of Biological Macromolecules, 253*, Article 126815.

Chen, X., Zhou, B., Gao, J., Wu, D., & Liang, H. (2022). EGCG-decorated zein complex particles: Relationship to synergistic interfacial properties. *Colloids and Surfaces A: Physicochemical and Engineering Aspects, 652*, Article 129879.

Fathi, M., Donsi, F., & McClements, D. J. (2018). Protein-based delivery systems for the nanoencapsulation of food ingredients. *Comprehensive Reviews in Food Science and Food Safety, 17*(4), 920–936.

Feng, W., Wang, R., Chen, Z., & Wang, T. (2019). Inhibition of aggregation of physically modified rice proteins by isoconcentration of l-Arg and l-Glu. *International Journal of Biological Macromolecules, 127*, 693–700.

Gao, X., Yao, Y., Wu, N., Xu, M., Zhao, Y., & Tu, Y. (2020). The sol-gel-sol transformation behavior of egg white proteins induced by alkali. *International Journal of Biological Macromolecules, 155*, 588–597.

Gómez-Guillén, M. C., Borderías, A. J., & Montero, P. (1997). Chemical interactions of nonmuscle proteins in the network of sardine (*Sardina pilchardus*) muscle gels. *LWT-Food Science and Technology, 30*(6), 602–608.

Gouda, M., Zhang, S., Liu, Y., Sheng, L., & Ma, M. (2017). Effects of four natural antioxidant phenyl terpenes on emulsifying and rheological properties of egg yolk. *LWT- Food Science and Technology, 83*, 59–67.

Guo, J., Zhou, Y., Yang, K., Yin, X., Ma, J., Li, Z., Sun, W., & Han, M. (2019). Effect of low-frequency magnetic field on the gel properties of pork myofibrillar proteins. *Food Chemistry, 274*, 775–781.

Han, X., Liang, Z., Tian, S., Liu, L., & Wang, S. (2022). Epigallocatechin gallate (EGCG) modification of structural and functional properties of whey protein isolate. *Food Research International, 158*, Article 111534.

Ji, F., Liu, H., Wang, C., Guo, N., Shen, Y., Luo, S., Jiang, S., & Zheng, Z. (2024). Remodeling the structure of soy protein fibrils to hydrogels for co-encapsulation of (−)-epigallocatechin gallate (EGCG) and curcumin: Role of EGCG. *Food Hydrocolloids, 147*, Article 109439.

Krupkova, O., Ferguson, S. J., & Wuertz-Kozak, K. (2016). Stability of (−)-epigallocatechin gallate and its activity in liquid formulations and delivery systems. *The Journal of Nutritional Biochemistry, 37*, 1–12.

Li, J., & Chen, Z. (2022). Fabrication of heat-treated soybean protein isolate-EGCG complex nanoparticle as a functional carrier for curcumin. *LWT- Food Science and Technology, 159*, Article 113059.

Li, J., Li, X., Wang, C., Zhang, M., Xu, Y., Zhou, B., Su, Y., & Yang, Y. (2018). Characteristics of gelling and water holding properties of hen egg white/yolk gel with NaCl addition. *Food Hydrocolloids, 77*, 887–893.

Li, X., Chen, L., Hua, Y., Chen, Y., Kong, X., & Zhang, C. (2020). Effect of preheating-induced denaturation during protein production on the structure and gelling properties of soybean proteins. *Food Hydrocolloids, 105*, Article 105846.

Liang, X., Ma, C., Yan, X., Zeng, H., McClements, D. J., Liu, X., & Liu, F. (2020). Structure, rheology and functionality of whey protein emulsion gels: Effects of double cross-linking with transglutaminase and calcium ions. *Food Hydrocolloids, 102*, Article 105569.

Liu, X., Wang, J., Huang, Q., Cheng, L., Gan, R., Liu, L., Wu, D., Li, H., Peng, L., & Geng, F. (2020). Underlying mechanism for the differences in heat-induced gel properties between thick egg whites and thin egg whites: Gel properties, structure and quantitative proteome analysis. *Food Hydrocolloids, 106*, Article 105873.

Luo, Q., Boom, R. M., & Janssen, A. E. (2015). Digestion of protein and protein gels in simulated gastric environment. *LWT- Food Science and Technology, 63*(1), 161–168.

Lv, Y., Chen, L., Wu, H., Xu, X., Zhou, G., Zhu, B., & Feng, X. (2019). (−)-Epigallocatechin-3-gallate-mediated formation of myofibrillar protein emulsion gels under malondialdehyde-induced oxidative stress. *Food Chemistry, 285*, 139–146.

Miao, L., Zhu, J., Peng, X., Feng, J., Dong, H., Tong, X., Wang, H., & Jiang, L. (2023). Effects of $CaCl_2$ concentration on fibrils formation and characteristics of soybean protein isolate and β-conglycinin/glycinin. *Food Hydrocolloids, 142*, Article 108769.

Monge-Morera, M., Lambrecht, M. A., Deleu, L. J., Gallardo, R., Louros, N. N., De Vleeschouwer, M., … Delcour, J. A. (2020). Processing induced changes in food proteins: Amyloid formation during boiling of hen egg white. *Biomacromolecules, 21*(6), 2218–2228.

Nagle, D. G., Ferreira, D., & Zhou, Y. D. (2006). Epigallocatechin-3-gallate (EGCG): Chemical and biomedical perspectives. *Phytochemistry, 67*(17), 1849–1855.

Razi, S. M., Fahim, H., Amirabadi, S., & Rashidinejad, A. (2023). An overview of the functional properties of egg white proteins and their application in the food industry. *Food Hydrocolloids, 135*, Article 108183.

Santos, Y. J. S., Facchinatto, W. M., Rochetti, A. L., Carvalho, R. A., Le Feunteun, S., Fukumasu, H., … Vanin, F. M. (2023). Systemic characterization of pupunha (*Bactris gasipaes*) flour with views of polyphenol content on cytotoxicity and protein in vitro digestion. *Food Chemistry, 405*, Article 134888.

Tan, C., Xu, Q. D., Chen, N., He, Q., Sun, Q., & Zeng, W. C. (2022). Cross-linking effects of EGCG on myofibrillar protein from common carp (*Cyprinus carpio*) and the action mechanism. *Journal of Food Biochemistry, 46*(12), Article e14416.

Wang, Y., Zhou, Y., Wang, X. X., Ma, F., Xu, B. C., Li, P. J., & Chen, C. G. (2020). Origin of high-pressure induced changes in the properties of reduced-sodium chicken myofibrillar protein gels containing $CaCl_2$: Physicochemical and molecular modification perspectives. *Food Chemistry, 319*, Article 126535.

Xiao, Y., Kang, S., Liu, Y., Guo, X., Li, M., & Xu, H. (2021). Effect and mechanism of calcium ions on the gelation properties of cellulose nanocrystals-whey protein isolate composite gels. *Food Hydrocolloids, 111*, Article 106401.

Xu, Y. Q., Yu, P., & Zhou, W. (2019). Combined effect of pH and temperature on the stability and antioxidant capacity of epigallocatechin gallate (EGCG) in aqueous system. *Journal of Food Engineering, 250*, 46–54.

Xue, H., Luo, X., Tu, Y., Zhao, Y., & Zhang, G. (2023). Amelioration of ovalbumin gel properties by EGCG via protein aggregation, hydrogen, and van der Waals force. *Food Chemistry, 422*, Article 136248.

Xue, H., Zhang, G., Han, T., Li, R., Liu, H., Gao, B., Tu, Y., & Zhao, Y. (2022). Improvement of gel properties and digestibility of the water-soluble polymer of tea polyphenol-egg white under thermal treatment. *Food Chemistry, 372*, Article 131319.

Yang, F., Zhang, M., Bhandari, B., & Liu, Y. (2018). Investigation on lemon juice gel as food material for 3D printing and optimization of printing parameters. *LWT- Food Science and Technology, 87*, 67–76.

Yao, L., Jiang, A., & Chen, L. (2020). Characterization of ethanol-induced egg white gel and transportation of active nutraceuticals. *LWT- Food Science and Technology, 130*, Article 109530.

Zeng, L., Ma, M., Li, C., & Luo, L. (2017). Stability of tea polyphenols solution with different pH at different temperatures. *International Journal of Food Properties, 20*(1), 1–18.

Zhang, S., Dongye, Z., Wang, L., Li, Z., Kang, M., Qian, Y., Chen, X., Ren, Y., & Chen, C. (2023). Influence of environmental pH on the interaction properties of WP-EGCG non-covalent nanocomplexes. *Journal of the Science of Food and Agriculture, 103*(11), 5364–5375.